

High-nuclearity, mixed-valence Mn_{17} , Mn_{18} and $\{\text{Mn}_{62}\}_n$ complexes from the use of triethanolamine†

Theocharis C. Stamatatos,^{‡*a} Dolos Foguet-Albiol,^a Wolfgang Wernsdorfer,^b Khalil A. Abboud^a and George Christou^{*a}

Received 2nd June 2010, Accepted 16th July 2010

DOI: 10.1039/c0cc01701a

The use of both azide and triethanolamine, with or without the presence of carboxylate groups, has provided new Mn_{17} , Mn_{18} and $\{\text{Mn}_{62}\}_n$ complexes with aesthetically-pleasing cage, layered, and linked-chain-type structures; two are also new single-molecule magnets.

One of the current challenges in inorganic chemistry is the synthesis and characterization of new molecular 3d metal polynuclear clusters at moderate oxidation states.¹ Reasons for this are varied, and not least among them is the aesthetic beauty that develops as the nuclearity of the clusters increases and the complexity of their molecular structures becomes apparent. From a more practical viewpoint, such large clusters can represent an alternative, ‘bottom-up’ route to nanoscale particles complementary to the traditional ‘top-down’ approach.² An example is the discovery that molecular 3d-metal clusters can function as magnets, providing a ‘bottom-up’ approach to nanoscale magnetic materials, and such individual molecular species have come to be known as single-molecule magnets (SMMs).³ SMMs are molecules that display slow magnetization relaxation below a blocking temperature, T_B , due to a large ground state spin (S) combined with a large Ising (easy-axis) magnetoanisotropy (negative zero-field splitting (zfs) parameter, D).³ In addition, SMMs are true ‘mesoscale’ particles straddling the classical/quantum interface, and thus display quantum properties such as quantum tunnelling of the magnetization vector (QTM)⁴ and quantum phase interference⁵ through the barrier. For all these reasons, SMMs have been proposed for various specialized applications, such as ultra-high density memory devices, spintronics, and quantum computing.⁶

Although complexes displaying SMM behaviour are known for several metals, manganese cluster chemistry continues to be the most fruitful source,⁷ giving a wide range of Mn_x nuclearities with x having values up to 84, the latter being the largest known SMM.^{7c} We have been developing new synthetic methods to Mn clusters of various nuclearities and

structural types, and have recently been exploring the use of N_3^- in higher oxidation state Mn chemistry in combination with various chelating/bridging ligands.⁸ From a magnetic viewpoint, the N_3^- ion bridging in the 1,1-fashion (end-on) is one of the strongest ferromagnetic mediators in molecular magnetism, and thus it constitutes an attractive route to new high-spin molecules and SMMs.^{8,9}

In the present work, we report Mn reactions with azides and the potentially tetradentate (N,O,O,O) triethanolamine (teaH_3) chelating/bridging group, which has previously been found a useful route to high nuclearity non-azido and some lower nuclearity azido-based metal clusters.^{10,11} We have been targeting higher nuclearity Mn products by exploring the reactions between teaH_3 , NaN_3 and various Mn reagents, with or without the co-presence of carboxylates. We herein report some results from this study, which has produced new mixed-valence Mn_{17} , Mn_{18} and $\{\text{Mn}_{62}\}_n$ molecular species with $\text{tea}^{3-}/\text{teaH}^{2-}/\text{N}_3^-$ and $\text{tea}^{3-}/\text{teaH}^{2-}/\text{N}_3^-/\text{RCO}_2^-$ ligand combinations.

The reaction of $\text{Mn}(\text{ClO}_4)_2 \cdot 6\text{H}_2\text{O}$, teaH_3 , NEt_3 , and NaN_3 in a 3 : 1 : 3 : 3 molar ratio in MeOH gave a dark brown solution from which was subsequently isolated $[\text{Mn}_{18}\text{O}_{11}(\text{OH})(\text{OMe})(\text{N}_3)_{12}(\text{tea})_3(\text{teaH})_3(\text{MeOH})]$ (**1**) in 65% yield.⁸ A very similar compound was recently reported by Murray and co-workers.¹¹ A similar reaction, but with pivalate, between $\text{Mn}(\text{ClO}_4)_2 \cdot 6\text{H}_2\text{O}$, $\text{NaO}_2\text{CCMe}_3$, teaH_3 , NEt_3 , and NaN_3 in a 1 : 2 : 1 : 1 : 2 ratio in MeCN/DMF (2 : 1, v/v) gave a similar dark brown solution from which was isolated $[\text{Mn}_{17}\text{NaO}_{10}(\text{OH})_2(\text{N}_3)_3(\text{O}_2\text{CCMe}_3)_{13}(\text{tea})_3(\text{teaH})(\text{DMF})]$ (**2**) in 45% yield. Interestingly, when $\text{Mn}(\text{ClO}_4)_2 \cdot 6\text{H}_2\text{O}$ and $\text{Mn}(\text{O}_2\text{CMe})_2 \cdot 4\text{H}_2\text{O}$ were combined in a 1 : 8 ratio in MeCN/MeOH (5 : 1, v/v), and treated with teaH_3 and NaN_3 in 1 : 4 ratio, the isolated product was now $[\text{Mn}_{31}\text{O}_{19}(\text{OH})(\text{OMe})_6(\text{N}_3)_4(\text{O}_2\text{CMe})_{23}(\text{tea})_2(\text{dea})_2(\text{MeOH})_2]_n$ (**3**) in 40% yield, where dea^{2-} is the dianion of diethanolamine. The partial transformation of teaH_3 to deaH_2 in **3** is attributed to metal-assisted $-(\text{CH}_2)_2\text{OH}$ bond cleavage processes¹² that are sometimes seen in 3d-metal cluster chemistry. The metal oxidation states and the protonation levels of O^{2-} , OH^- , OMe^- , $\text{tea}^{3-}/\text{teaH}^{2-}$, and dea^{2-} O atoms in **1–3** were established by Mn/Na and O bond valence sum (BVS) calculations,^{13,14} inspection of metric parameters, and detection of Mn^{III} Jahn–Teller (JT) elongation axes.

The structure§ of **1** consists of a mixed-valent ($\text{Mn}^{\text{II}}_3\text{Mn}^{\text{III}}_{15}$) Mn_{18} cage (Fig. 1, left) with a ‘pyramid’ or ‘cone’-like topology.¹⁴ The eight $\mu_4\text{-O}^{2-}$, three $\mu_3\text{-O}^{2-}$, one $\mu_3\text{-OH}^-$, and one $\mu_3\text{-OMe}^-$ ions hold the core together, as well as chelating/bridging $\text{tea}^{3-}/\text{teaH}^{2-}$ and both terminal and

^a Department of Chemistry, University of Florida, Gainesville, Florida 32611-7200, USA

^b Institut Néel, CNRS & Université J. Fourier, BP-166, Grenoble, Cedex 9, France

† Electronic supplementary information (ESI) available: Crystallographic data (CIF format) for **1**·2CH₂Cl₂·4Et₂O, **2**·5MeCN and **3**·26MeCN, synthetic details for the **1–3**, and various structural and magnetism figures. CCDC 700136–700138. For ESI and crystallographic data in CIF or other electronic format see DOI: 10.1039/c0cc01701a

‡ Present address: Department of Chemistry, University of Patras, Patras 26504, Greece. E-mail: thstama@chemistry.upatras.gr; Fax: +30-2610-997118; Tel.: +30-2610-996020.

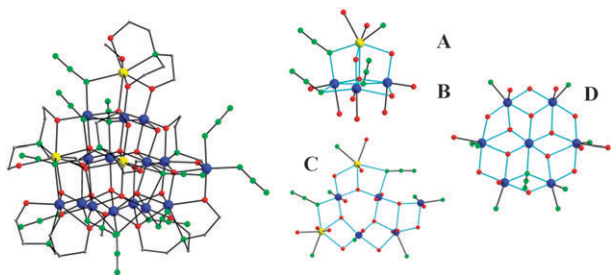


Fig. 1 Structure of **1** (left) and the four layers of its core (right). H atoms have been omitted for clarity. Colour scheme: Mn^{II} yellow; Mn^{III} blue; O red; N green; C grey.

bridging azide groups. The core of **1** can be conveniently dissected into four layers, ABCD, of different sizes (Fig. 1, right) but all comprising fused [Mn₃O] triangular units: the Mn^{II} monomeric layer A is the apex of the Mn₁₈ 'cone', linked to layer B which is a Mn^{III}₃ triangle, thus giving a combined-layer AB tetrahedral topology; layer C is a large Mn^{II}₂Mn^{III}₄ triangle comprising three corner-sharing Mn^{II}Mn^{III}₂ and Mn^{III}₃ triangles connected to an additional, extrinsic Mn^{III} atom; and layer D consists of a Mn^{III}₇ disk-like unit. Each layer is held together and linked to neighbouring layers by a combination of oxide, alkoxide, and μ₃-1,1,1 or μ-1,1 (end-on) azide ligands. The three tea³⁻ and teaH²⁻ groups are of four types: η³:η¹:η²:η²:μ₅ and η¹:η¹:η³:η²:μ₄ for the former, and η²:η¹:η³:η¹:μ₄ and η²:η¹:η²:η¹:μ₃ for the latter,¹⁴ reflecting the bridging flexibility of the triethanolamine group.

The structure of **2** (Mn^{II}₄Mn^{III}₁₂Mn^{IV}) consists of a Mn₁₇Na cage-like cluster (Fig. 2, top) with an irregular topology. The [Mn₁₇Na(μ₄-O)₈(μ₃-O)₂(μ₃-OH)(μ-OH)₂(μ₃-N₃)]²⁵⁺ core (Fig. 2, bottom) comprises seven [Mn₄(μ₄-O²⁻)] and one [Mn₃Na(μ₄-O²⁻)] tetrahedra fused together and linked to one adjacent [Mn₂Na(μ₃-OH⁻)] and two [Mn₃(μ₃-O²⁻)] triangles

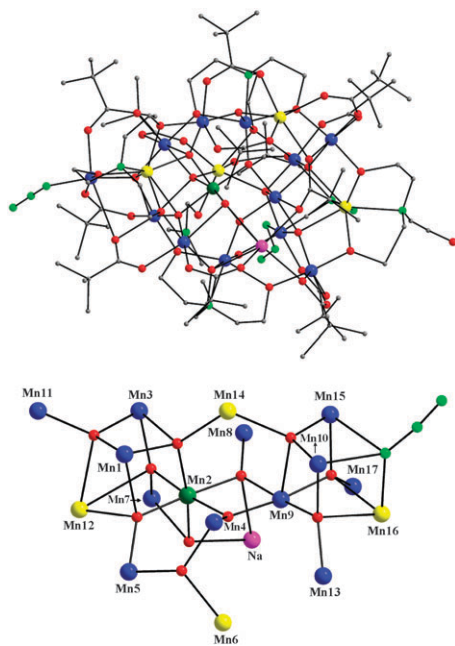


Fig. 2 Structure of complex **2** (top) and its core (bottom). Colour scheme: Mn^{II} yellow; Mn^{III} blue; Mn^{IV} olive; Na purple; O red; N green; C grey.

by common Mn vertices. The core can also be described as a central [Mn₃Na(μ₄-O²⁻)] tetrahedron fused to [Mn₄(μ₃-O²⁻)₄] and [Mn₄(μ₃-O²⁻)₃(μ₃-N₃)] cubanes at common atoms Mn(2) and Mn(9), respectively. All μ₃-O²⁻ ions in each cubane convert to a μ₄ mode and bridge seven adjacent Mn atoms, three of which (Mn2,5,7) are fused to the corresponding triangular subunits. The three tea³⁻ groups are each bridging up to six Mn atoms, acting as η³:η¹:η²:η³:μ₆, η²:η¹:η³:η²:μ₅ and η²:η¹:η²:η²:μ₃ ligands, the μ₆ mode being seen for a first time in the coordination chemistry of this group, while the only teaH²⁻ group is bridging in a η²:η¹:η²:μ₃ mode.¹⁴ Peripheral ligation is provided by ten η¹:η¹:μ, two η¹:η²:μ and an η²:η²:μ₄ Me₃CCO₂⁻ groups, as well as two terminal N₃⁻ ions and a terminal DMF molecule.

The structure of **3** (Mn^{II}₁₁Mn^{III}₂₀) consists of Mn₂₈ units comprising a central Mn₁₄ subunit attached on each side to a Mn₄ rhombus and a Mn₃ triangle, with the metal atoms bridged by oxo, alkoxo, azido and acetato ions. These Mn₂₈ units are connected by linear [Mn^{II}₃(O₂CMe)₅(N₃)] units into a 1D zig-zag chain. The structure is at first glance a polymer of Mn₃₁ units, but the Mn₃ bridge in a way that makes adjacent Mn₂₈ inequivalent, and complex **3** is thus best described as a chain of repeating Mn₆₂ units (Fig. 3) of formula [Mn₆₂O₃₈(OH)₂(OMe)₁₂(N₃)₈(O₂CMe)₄₆(tea)₄(dea)₄(MeOH)₄]_n. Further, the 1D chains are linked by Mn(14)-N₃-Mn(18) inter-chain bridges, with the azide in an end-to-end mode, giving a 3D covalent network. The packing of the chains is provided in Fig. S11 (ESI[†]) which shows that (i) the linked-chains give sheets with a herring-bone pattern, and (ii) chains of adjacent linked-sheets are staggered so that when viewed along the chain axes a hexagonal close-packing is observed.

Solid-state dc (direct current) magnetic susceptibility (χ_M) data were collected on **1**, **2**, and **3**·10MeCN in a 1 kG (0.1 T) field in the 5.0–300 K range. The data are plotted as χ_MT vs. T in Fig. S3 (ESI[†]), and both **1** and **2** clearly have relatively large ground-state spin (*S*) values, whereas **3**·10MeCN is strongly antiferromagnetically-coupled with χ_MT heading for 0 cm³ K mol⁻¹ at 0 K, indicating a diamagnetic ground state. χ_MT for **1** increases from 66.53 cm³ K mol⁻¹ at 300 K to 75.40 cm³ K mol⁻¹ at 100.0 K, and then decreases to a plateau of ~60.50 cm³ K mol⁻¹ at 15.0–8.0 K, before dropping to 58.93 cm³ K mol⁻¹ at 5.0 K; the decrease at the lowest temperatures is assigned to Zeeman effects, zero-field splitting and/or weak intermolecular interactions. For **2**, χ_MT steadily decreases from 44.74 cm³ K mol⁻¹ at 300 K to a plateau of

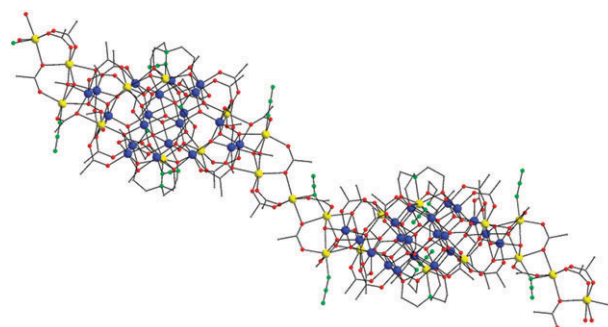


Fig. 3 Structure of the repeating {Mn₆₂} unit of polymeric complex **3**. Colour scheme as in Fig. 1.

$\sim 35.50 \text{ cm}^3 \text{ K mol}^{-1}$ at 40.0–20.0 K, before dropping to $33.49 \text{ cm}^3 \text{ K mol}^{-1}$ at 5.0 K. The $\chi_M T$ plateau values for **1** and **2** suggest ground-state spin values, S , of 21/2 and 17/2, respectively; the spin-only ($g = 2$) values are 60.38 and $40.38 \text{ cm}^3 \text{ K mol}^{-1}$, respectively.

To determine the ground states of **1** and **2**, magnetization (M) data were collected in the 0.1–1.0 T and 1.8–10.0 K ranges, and these are plotted as $M/N\mu_B$ vs. H/T in Fig. S4 and S5 (ESI[†]), respectively. The data were fit by matrix-diagonalization to a model that assumes only the ground state is populated, includes axial zero-field splitting and the Zeeman interaction, and carries out a full powder average. The best fit (solid lines in Fig. S4 and S5, ESI[†]) gave $S = 21/2$, $g = 1.99(3)$ and $D = -0.073(5) \text{ cm}^{-1}$ for **1** and $S = 17/2$, $g = 1.95(1)$ and $D = -0.218(5) \text{ cm}^{-1}$ for **2**. Alternative fits with $S = 19/2$ or $23/2$ for **1** and $15/2$ or $19/2$ for **2** were rejected because they gave unreasonable values of g . We conclude that **1** and **2** have $S = 21/2$ and $17/2$ ground states, respectively. This was further confirmed by ac (alternating current) susceptibility studies.¹⁴

The $S = 21/2$ and $17/2$ ground states and negative D values suggest that both **1** and **2** might be SMMs. At temperatures < 3.0 K, frequency-dependent tails of out-of-phase (χ_M'') ac susceptibility signals for both complexes were observed.¹⁴ Such signals are an indication of the superparamagnetic-like slow relaxation of an SMM. To confirm this, magnetization vs. applied dc field data down to 0.04 K were collected on single-crystals using a micro-SQUID apparatus.¹⁵ Both complexes exhibit hysteresis loops below ~ 1.0 K whose coercivities increase with increasing field sweep rate¹⁴ and decreasing temperature (Fig. 4), confirming **1** and **2** to be new Mn SMMs. Arrhenius plots were constructed from combined ac χ_M'' data and dc magnetization decay data, giving $U_{\text{eff}} = 6.1 \text{ cm}^{-1} = 8.8 \text{ K}$ and $\tau_0 = 10^{-7} \text{ s}$ for **1** and $U_{\text{eff}} = 13.2 \text{ cm}^{-1} = 19.0 \text{ K}$ and $\tau_0 = 10^{-11} \text{ s}$ for **2**, where τ_0 is the pre-exponential factor.¹⁴

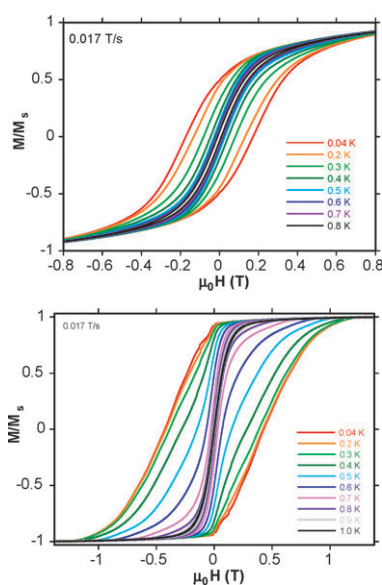


Fig. 4 Magnetization (M) vs. applied dc field (H) hysteresis loops for **1-2CH₂Cl₂·4Et₂O** (top) and **2-5MeCN** (bottom) at the indicated temperatures. M is normalized to its saturation value (M_s).

Such ranges in τ_0 values for high-nuclearity SMMs are becoming more common, and can be assigned to differing factors such as relaxation contributions through low-lying excited states, distribution of molecular environments, and weak intermolecular interactions.

In conclusion, azide and triethanolamine groups together, with or without the presence of carboxylate anions, have provided three Mn clusters with interesting structures, namely a multi-layer pyramid (**1**), a closed cage (**2**) and a zig-zag chain (**3**), two of which (**1** and **2**) are also new members of the SMM family. These three complexes establish the potential of this reaction system to continue giving new molecular species with unprecedented nuclearities in 3d-metal coordination chemistry.

This work was supported by the National Science Foundation (CHE-0910472).

Notes and references

§ Crystal data for **1-2CH₂Cl₂·4Et₂O**: $C_{56}H_{127}Cl_4Mn_{18}N_{42}O_{36}$, $M_w = 3095.72$, triclinic, space group $P1$, $a = 15.3132(2) \text{ \AA}$, $b = 18.3122(11) \text{ \AA}$, $c = 21.422(2) \text{ \AA}$, $\alpha = 68.092(2)^\circ$, $\beta = 79.91(2)^\circ$, $\gamma = 74.134(2)^\circ$, $V = 5342.9(6) \text{ \AA}^3$, $Z = 2$, $\rho_{\text{calcd}} = 1.924 \text{ g cm}^{-3}$, $T = 173(2) \text{ K}$, 35 186 reflections collected, 23 378 unique ($R_{\text{int}} = 0.0433$), $R1 [I > 2\sigma(I)] = 0.0577$, $wR2 = 0.1433$ (F^2 , all data). CCDC 700137. Crystal data for **2-5MeCN**: $C_{102}H_{188}Mn_{17}NaN_{19}O_{51}$, $M_w = 3453.68$, orthorhombic, space group $P2_12_12_1$, $a = 17.463(3) \text{ \AA}$, $b = 18.144(3) \text{ \AA}$, $c = 46.054(7) \text{ \AA}$, $V = 46.054(7) \text{ \AA}^3$, $Z = 4$, $\rho_{\text{calcd}} = 1.572 \text{ g cm}^{-3}$, $T = 173(2) \text{ K}$, 55 542 reflections collected, 19 027 unique ($R_{\text{int}} = 0.1192$), $R1 [I > 2\sigma(I)] = 0.0972$, $wR2 = 0.2053$ (F^2 , all data). CCDC 700136. Crystal data for **3-26MeCN**: $C_{126}H_{215}Mn_{31}N_{42}O_{84}$, $M_w = 5365.54$, monoclinic, space group $P2_1/c$, $a = 35.759(4) \text{ \AA}$, $b = 14.8904(16) \text{ \AA}$, $c = 32.943(4) \text{ \AA}$, $\beta = 92.562(2)^\circ$, $V = 17 524(3) \text{ \AA}^3$, $Z = 4$, $\rho_{\text{calcd}} = 2.034 \text{ g cm}^{-3}$, $T = 173(2) \text{ K}$, 69 613 reflections collected, 22 840 unique ($R_{\text{int}} = 0.1113$), $R1 [I > 2\sigma(I)] = 0.0776$, $wR2 = 0.1874$ (F^2 , all data). CCDC 700138.

- 1 E. G. Mednikov and L. F. Dahl, *Small*, 2008, **4**, 534.
- 2 G. Schmid, *Nanoparticles—From Theory to Application*, Wiley-VCH, Weinheim, 2005, vol. 19, p. 7.
- 3 D. Gatteschi and R. Sessoli, *Angew. Chem., Int. Ed.*, 2003, **42**, 268.
- 4 J. R. Friedman, M. P. Sarachik, J. Tejada and R. Ziolo, *Phys. Rev. Lett.*, 1996, **76**, 3830.
- 5 W. Wernsdorfer and R. Sessoli, *Science*, 1999, **284**, 133.
- 6 L. Bogani and W. Wernsdorfer, *Nat. Mater.*, 2008, **7**, 179.
- 7 (a) E. K. Brechin, *Chem. Commun.*, 2005, 5141; (b) R. T. W. Scott, S. Parsons, M. Murugesu, W. Wernsdorfer, G. Christou and E. K. Brechin, *Angew. Chem., Int. Ed.*, 2005, **44**, 6540; (c) A. J. Tasiopoulos, A. Vinslava, W. Wernsdorfer, K. A. Abboud and G. Christou, *Angew. Chem., Int. Ed.*, 2004, **43**, 2117.
- 8 Th. C. Stamatatos and G. Christou, *Inorg. Chem.*, 2009, **48**, 3308.
- 9 A. Escuer and G. Aromi, *Eur. J. Inorg. Chem.*, 2006, 4721.
- 10 (a) M. Murugesu, W. Wernsdorfer, K. A. Abboud and G. Christou, *Angew. Chem., Int. Ed.*, 2005, **44**, 892; (b) Th. C. Stamatatos, D. Foguet-Albiol, K. M. Poole, W. Wernsdorfer, K. A. Abboud, T. A. O'Brien and G. Christou, *Inorg. Chem.*, 2009, **48**, 9831; (c) S. K. Langley, B. Moubaraki, K. J. Berry and K. S. Murray, *Dalton Trans.*, 2010, 4848; (d) L. M. Wittick, L. F. Jones, P. Jensen, B. Moubaraki, L. Spiccia, K. J. Berry and K. S. Murray, *Dalton Trans.*, 2006, 1534; (e) Th. C. Stamatatos, K. M. Poole, D. Foguet-Albiol, K. A. Abboud, T. A. O'Brien and G. Christou, *Inorg. Chem.*, 2008, **47**, 6593.
- 11 S. K. Langley, K. J. Berry, B. Moubaraki and K. S. Murray, *Dalton Trans.*, 2009, 973.
- 12 S. Horikoshi, N. Watanabe, M. Mukae, H. Hidaka and N. Serpone, *New J. Chem.*, 2001, **25**, 999.
- 13 W. Liu and H. H. Thorp, *Inorg. Chem.*, 1993, **32**, 4102.
- 14 See the ESI[†].
- 15 W. Wernsdorfer, *Adv. Chem. Phys.*, 2001, **118**, 99.